Open Access Library Journal
2026, Volume 13, e14984
ISSN Online: 2333-9721
ISSN Print: 2333-9705

Research on the Application of Nitrogen Removal Technology for Rural Sewage Based on Embedded Fillers

Yaokun Zhang, Hong Yang*

Key Laboratory of Beijing for Water Quality Science and Water Environmental Recovery Engineering, College of Architectural Engineering, Beijing University of Technology, Beijing, China
Email: *yhong@bjut.edu.cn

How to cite this paper: Zhang Y.K. and Yang, H. (2026) Research on the Application of Nitrogen Removal Technology for Rural Sewage Based on Embedded Fillers. *Open Access Library Journal*, **13**: e14984.
https://doi.org/10.4236/oalib.1114984

Received: February 4, 2026
Accepted: March 8, 2026
Published: March 11, 2026

Abstract

China's rural sewage has the characteristics of large fluctuation of water quality and quantity, low carbon-nitrogen ratio, and low treatment efficiency of traditional processes at low temperature, which is difficult to meet the treatment needs. In this study, Microbial Immobilization Technology (MIT) was used to prepare immobilized biological fillers to improve the operation stability and treatment efficiency of the system under low temperature conditions. Based on the existing rural sewage collection tank reconstruction test device (design capacity 3 m^3/h), the system treatment efficiency at 8˚C - 19.3˚C was investigated, and the microbial community structure was analyzed by high-throughput sequencing. The results showed that the average removal rate of NH_4^+-N was 93.43% and the average removal rate of COD was 82.25% in the low temperature cycle. The effluent concentrations were 0.65 mg/L and 24.97 mg/L, respectively. The effluent quality was better than the Class IV standard of "Surface Water Environmental Quality Standard" (GB3838-2002). The microbial community structure was highly matched with the process function. The microbial community analysis showed that the dominant bacteria in each functional pool in the embedded filler were clear, the structure was stable, and good metabolic activity was maintained under low temperature conditions. The embedded filler exhibits high biological activity and stress resistance. This study provides theoretical support and engineering reference for the practical application of microbial embedding immobilization technology in low-temperature rural sewage treatment.

Subject Areas

Civil Engineering

Keywords

Rural Sewage, Low Temperature, Embedding Immobilization Technology, Practical Application

1. Introduction

Currently, China has made positive progress in treating rural domestic wastewater, with a national treatment rate exceeding 45% by the end of 2024[1]. However, deficiencies still exist in rural wastewater treatment, including incomplete collection systems, substandard treatment effectiveness, non-compliant discharges, and unstable operation [2]-[5]. The "Five-Year Action Plan for the Improvement and Enhancement of Rural Living Environment (2021-2025)" requires accelerating rural domestic wastewater treatment, adapting measures to local conditions, and focusing on rural toilet revolution, domestic wastewater and garbage treatment, and village appearance improvement [6]. To advance the "15th Five-Year Plan" and accelerate the "construction of a new development pattern" and the integrated management of mountains, rivers, forests, fields, lakes, grasses, and sands, it is necessary to accelerate rural wastewater treatment.

Rural wastewater has characteristics significantly different from urban wastewater [7]-[9]: 1) Large fluctuations in water quality and quantity, significantly influenced by villagers' living habits and seasonal water usage patterns; 2) Low carbon-to-nitrogen ratio (C/N), generally in the range of 3.8 - 5.0, limiting the efficiency of nitrogen removal processes; 3) If discharged directly without effective treatment, it can easily cause eutrophication of rural water bodies and soil pollution. Traditional wastewater treatment processes are difficult to adapt to the characteristics of rural wastewater. For example, the activated sludge process experiences significant instability during flow fluctuations [10]; under low C/N conditions, substantial external carbon source addition is required to maintain denitrification efficiency [11]; and winter low temperatures (≤13˚C) cause a sharp decline in the biological activity of activated sludge [12], making it difficult to guarantee effluent quality. While constructed wetlands are suitable for decentralized rural wastewater treatment, they require pre-treatment and process adjustment, and their adaptability to low temperatures remains limited, especially in northern winters [13]-[15]. Additionally, they require large land areas, and many villages lack the land conditions for wetland construction.

To overcome these challenges, embedded immobilized biological fillers prepared using Microbial Immobilization Technology (MIT) offer an effective method. MIT involves fixing enriched and selected functional microbial communities within the gel of the filler, providing a stable growth environment [16]. Compared to the traditional activated sludge process, it offers greater stability due to the absence of sludge washout issues, higher biomass, and better resistance to environmental changes [17] [18]. More critically, it exhibits high biochemical efficiency

and small footprint.

This experiment relies on MIT to explore the optimal operating conditions for embedded immobilized biological fillers under low temperatures, given the aforementioned characteristics of rural wastewater. It examines the operational status of the fillers in the hydrolysis-acidification tank, denitrification tank, and short-cut nitrification tank, and analyzes the community characteristics and synergistic effects of the microbial communities. The aim is to provide references for the practical application of embedded immobilized biological fillers.

2. Materials and Methods

2.1. Test Setup and Operation Mode

The device was upgraded based on an existing collection tank structure, using concrete partitions placed within the original tank. The plane dimensions were 5.0 × 5.0 m^2, with a tank depth of 4.7 m, as shown in Figure 1. The designed wastewater treatment capacity was 3 m^3/h. From front to back, the compartments were: screen tank, inlet tank, hydrolysis-acidification tank, primary denitrification tank, partial nitrification tank, secondary denitrification tank, anaerobic phosphorus removal tank, aerobic phosphorus removal tank, effluent sedimentation tank, and disinfection tank (See Table 1).

The tanks were separated by concrete walls. Wastewater passed through a screen mesh with 50 mm × 50 mm openings. Aeration pipes were installed at the bottom of the anaerobic hydrolysis-acidification tank, primary denitrification

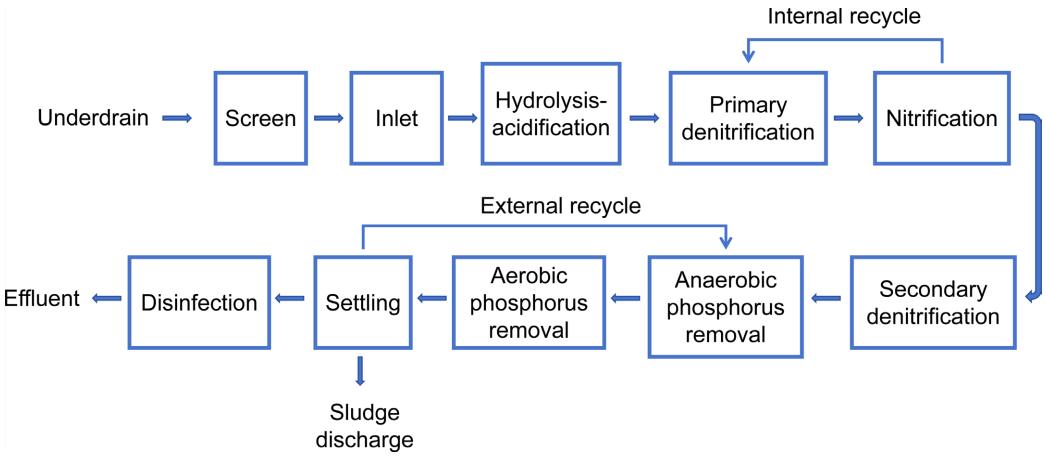

Figure 1. Sewage tank test flow chart.

Table 1. The design parameters of each pool of the test pool.

Design Tank	Anaerobic Hydrolysis-Acidification	Primary Denitrification	Partial nitrification	Secondary Denitrification	Anaerobic Phosphorus Removal	Aerobic Phosphorus Removal
Area (m^2)	1.5	1.5	4.0	1.1	0.75	0.75
HRT (h)	2.5	2.5	6.6	1.8	1.25	1.25

tank, secondary denitrification tank, and anaerobic phosphorus removal tank for backwashing the immobilized fillers. Three sets of fine bubble aerators (3 sets × 4 units, diameter 300 mm) were installed at the bottom of the partial nitrification tank to supply oxygen and provide mixing. Based on online monitoring by a fluorescence-based dissolved oxygen probe, intermittent aeration was achieved by controlling the Roots blower to automatically start/stop within a preset DO range. One set of fine bubble aerators (1 set × 2 units, diameter 300 mm) was installed at the bottom of the aerobic phosphorus removal tank to supply oxygen for aerobic phosphorus-removing microorganisms. The internal recycle ratio was adjusted by the flow rate of the internal recycle pump at the end of the partial nitrification tank. Sludge was recycled (and also wasted) by a sludge return pump. The treatment system had no discharge pipeline. With effluent COD ≤ 30 mg/L, and according to the "Standards for Irrigation Water Quality" (GB 5084-2021), which requires COD ≤ 200 mg/L for irrigating dryland crops, the treated effluent met agricultural irrigation standards. Currently, all treated effluent was used for nearby woodland irrigation (See Table 2).

Table 2. Test operation parameters.

Stage	Time/d	Average NH_4^+-N /(mg·L^{-1})	Average COD/(mg·L^{-1})	Recycle Ratio (%)	DO (mg/L)
I	1 - 49	29.92	135.59	100	3 - 4
II	50 - 150	36.89	163.59	150	3.8 - 5

2.2. Preparation of Immobilized Biofillers and Wastewater Sources

According to the "Division of Climatic Seasons" (GB/T 42074-2022), the winter start date for 2024 was determined to be November 4. Taking this date (November 1, 2024) as the start of the low-temperature period, statistics were collected until March 31, 2025, totaling 149 days. The water temperature in the aerobic nitrification tank ranged from 8˚C to 19.3˚C.

The test water was collected via the rural drainage network system, passed through the screen mesh in the test tank for pre-treatment, and then directly entered the raw water tank. It was then lifted by an inlet pump into the hydrolysis-acidification tank. As the test water was rural wastewater, it exhibited the characteristics of low C/N ratio and unstable flow. During the 150-day test period, the average influent NH_4^+-N concentration was 33.4 mg/L, and the average COD concentration was 150 mg/L.

The embedded immobilized fillers used in the experiment were all prepared using polyvinyl alcohol (PVA) gel as the carrier. The specific preparation process was as follows: A 20% (w/w) PVA solution cooled to about 35˚C was mixed proportionally with sludge enriched and cultured in an industrial fermenter. Subsequently, diatomaceous earth, $CaCO_3$, and powdered activated carbon were added and stirred evenly. The mixed material was processed by a laboratory-designed

forming device or specific molds into hollow ring structures with a diameter of 10 mm and a thickness of 3 mm. Then, cross-linking and solidification were performed in a saturated boric acid solution, followed by stabilization treatment in a Na_3PO_4 solution. Finally, the formed fillers were loaded into polypropylene plastic balls with a diameter of 80 mm to create immobilized filler balls for the experiment.

To enable confident interpretation of the reported averages, a water-quality sampling plan was implemented. Samples were collected at each process node as illustrated in **Figure 1** (e.g., influent, effluent of each functional tank), rather than at fixed time intervals, to capture the performance of individual units along the treatment train. All samples were grab samples. For quality assurance/quality control (QA/QC), the dissolved oxygen (DO) probe was calibrated weekly using the manufacturer's two-point calibration method. Duplicate samples were analyzed for 10% of the total samples, and the relative percent difference was consistently below 5%. Blank samples (deionized water) were analyzed daily to check for contamination. The method detection limits for NH_4^+-N, NO_2^--N, NO_3^--N, and COD were 0.025 mg/L, 0.003 mg/L, 0.02 mg/L, and 5 mg/L, respectively. The practical quantification limits were set at ten times the detection limits.

The immobilized embedded fillers used in the experiment were all immobilized using polyvinyl alcohol (PVA) gel. The detailed preparation procedure is as follows: The PVA-embedded fillers were fabricated by mixing a PVA solution (20%, w/w) with concentrated seed sludge having a moisture content of 95%. $CaCO_3$ (18 g/L) and powdered activated carbon (38 g/L) were added separately and stirred. The mixture was then processed into a hollow ring structure (diameter: 10 mm, thickness: 3 mm) using an in-house designed and developed embedding molding apparatus. Cross-linking and stabilization were subsequently performed in saturated H_3BO_3 solution and Na_3PO_4 solution. Finally, the embedded fillers were packed into polypropylene plastic spheres with a diameter of 80 mm to obtain the final filler spheres used in the experiment.

The immobilized fillers were loaded into hollow plastic floating balls with a diameter of 80 mm. The bulk volume of the fillers within each ball accounted for approximately 40% - 50% of the effective volume of the ball. This loading rate was maintained consistently across all functional tanks (hydrolysis-acidification, denitrification, and nitrification tanks).

To prevent clogging and maintain long-term biological activity, the filler balls were backwashed regularly. The backwashing was performed using a combination of air and water scouring for approximately 40 minutes per event, with a frequency of once every one to two weeks, depending on the observed pressure drop and visual inspection of biofilm accumulation.

2.3. Water Quality Analysis

Total Inorganic Nitrogen (TIN) was calculated as the sum of NH_4^+-N, NO_2^--N and NO_3^--N. The "total nitrogen removal contribution (65%)" for the primary

denitrification tank was calculated as the percentage of TIN removed in that tank relative to the total TIN removed by the entire system (including assimilation and denitrification in all tanks).

Water quality indicators at the inlet and outlet of the partial nitrification and denitrification reactors were measured periodically. According to relevant standards in "Water and Wastewater Monitoring and Analysis Methods" (Fourth Edition): NH_4^+-N was measured by Nessler's reagent spectrophotometry; NO_2^--N by N-(1-naphthyl)-ethylenediamine spectrophotometry; NO_3^--N by ultraviolet spectrophotometry. COD was measured using a Lianhua Technology COD rapid analyzer [19], and DO was measured using a Hach HQ30D portable DO meter.

2.4. Calculation Formulas

NAR (Nitrite Accumulation Rate) and AOR (Ammonia Oxidation Rate, mg/(L·h)) were calculated using the following formulas:

$$\mathrm{NAR}(\%) = \frac{NO_2^- - N_{eff}}{NO_2^- - N_{eff} + NO_3^- - N_{eff}} \times 100\% \quad (1)$$

$$\mathrm{AOR}\left(\mathrm{mg}/(\mathrm{L}\cdot\mathrm{h})\right) = \frac{NH_4^+ - N_{inf} - NH_4^+ - N_{eff}}{\mathrm{HRT}} \quad (2)$$

where: NAR: Nitrite Accumulation Rate (%); AOR: Ammonia Oxidation Rate (mg/(L·h)); NO_2^--N_{eff}: Effluent nitrite nitrogen concentration (mg/L); NO_3^--N_{eff} Effluent nitrate nitrogen concentration (mg/L).

2.5. Microbial Analysis

On March 31, 2025, the last day of the system's low-temperature operation, embedded fillers were taken as representative samples from the hydrolysis-acidification tank, primary denitrification tank, and partial nitrification tank to analyze changes in microbial community structure during long-term operation. Samples were sent to Shanghai Majorbio Bio-pharm Technology Co., Ltd. for microbial diversity analysis. Analysis process: 1) Total DNA was extracted using the Omega Soil DNA Kit; 2) PCR amplification was performed using primers targeting the V3-V4 region of the 16S rRNA gene (338F: 5'-ACTCCTACGGGAGGCAGCAG-3'; 806R: 5'-GGACTACHVGGGTWTCTAAT-3'); 3) Amplified products were purified and subjected to high-throughput sequencing on the Illumina MiSeq platform; 4) Sequencing data were processed on the Majorbio Cloud Platform for OTU clustering, species annotation, and diversity analysis.

2.6. Site Photos

As shown in **Figure 2**, this is a photo taken at the scene.

3. Results and Discussion

Compared to urban wastewater treatment plants where the minimum winter water temperature is 13˚C - 16˚C, the minimum winter water temperature in north-

ern rural areas is below 10˚C. This is due to the use of drain valves in rural areas during winter to prevent pipe freezing, resulting in higher flow rates and lower temperatures.

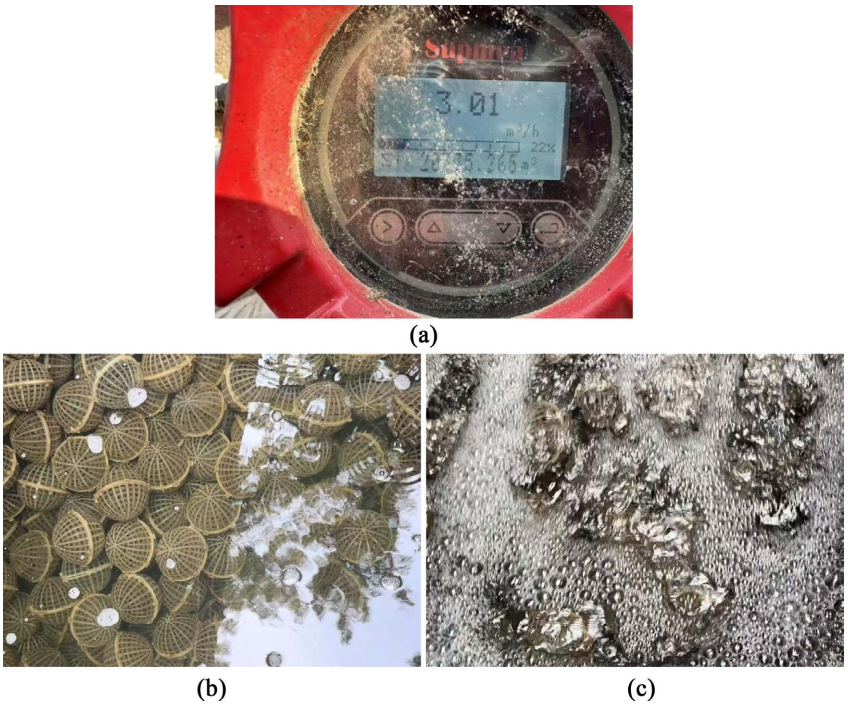

Figure 2. Part of the scene photos. (a) Flow meter; (b) Nitrification tank in non-aeration state; (c) Nitrification tank in aeration state.

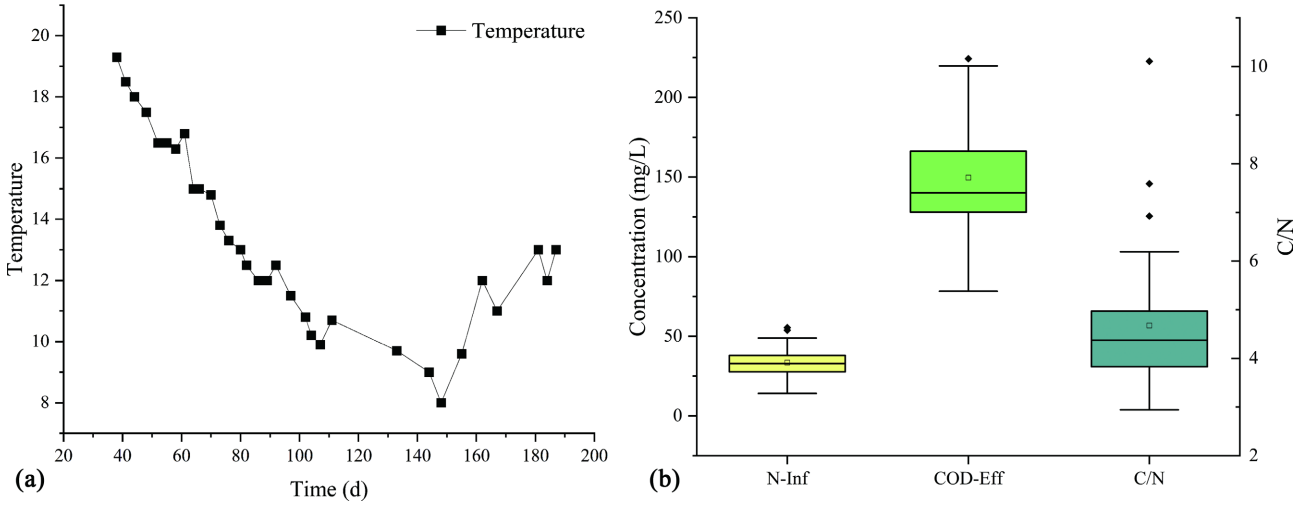

Figure 3. The water temperature line and influent water quality in the test stage. (a)Water temperature curve; (b) Influent water quality.

This experiment recorded field data starting from November 1, 2024. According to **Figure 3**, the influent NH_4^+-N concentration ranged from 27.71 to 37.98 mg/L, and influent COD ranged from 127.97 to 166.30 mg/L, with a C/N ratio between 3.8 and 5, classifying it as low C/N wastewater [20].

3.1. Nitrification Performance in Winter

To study the low-temperature resistance of the immobilized biological fillers in actual rural wastewater during winter, Figure 4 shows the changes in influent and effluent water quality. Among the collected water samples, the lowest temperature reached 8˚C. Figure 4 demonstrates the good treatment performance of the wastewater treatment tank: average NH_4^+-N removal rate was 93.43%, average NO_2^--N accumulation rate was 82.8%, average COD removal rate was 82.25%, average effluent NH_4^+-N was 0.65 mg/L, and average effluent COD was 24.97 mg/L. This indicates that the biological fillers maintained good biological activity under winter low-temperature conditions. The effluent quality met and surpassed the Class IV standard of the "Environmental Quality Standards for Surface Water" (GB3838-2002), and exceeded the Beijing local discharge standard Level A (DB11/1612-2019).

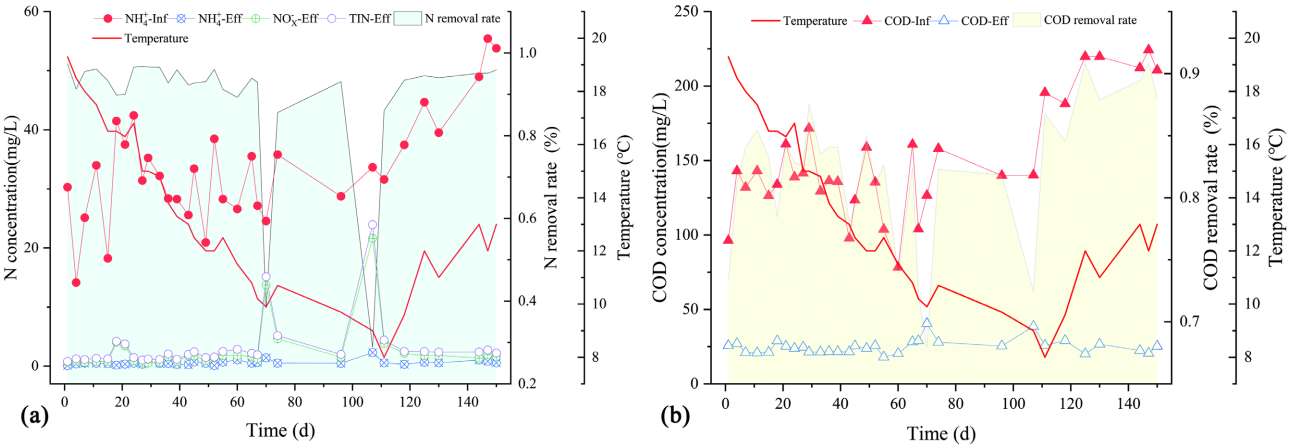

Figure 4. Change of water quality in and out of the system.

3.1.1. Denitrification Performance in Winter

Figure 5 shows a cross-sectional view of the nitrification tank. According to Figure 5, the internal structure of the nitrification tank can be seen more intuitively, and it serves as an equipment diagram for this experiment.

According to the aforementioned standard, on day 1 when the water temperature was still 19.3˚C, the NH_4^+-N concentration in the nitrification tank effluent was 0.32 mg/L, the nitrite accumulation rate (NAR) was 83.88%, and the system effluent NH_4^+-N was 0.1 mg/L, far below the Class IV water standard (of China's GB 3838-2002). As the temperature decreased, the system effluent NH_4^+-N in the partial nitrification tank did not show significant fluctuations. This might be because the AOB population remained dominant as the water temperature slowly decreased, consistent with the research by W Ai *et al.* [21], which could enhance resistance to temperature. However, on day 55 when the water temperature was 12.5˚C, the system effluent NH_4^+-N was 0.67 mg/L, and NAR decreased to 79.44%. By day 74, the average system effluent NH_4^+-N was 0.52 mg/L > 0.5 mg/L, and the average system NH_4^+-N removal rate decreased from 98.57% to 97.11%.

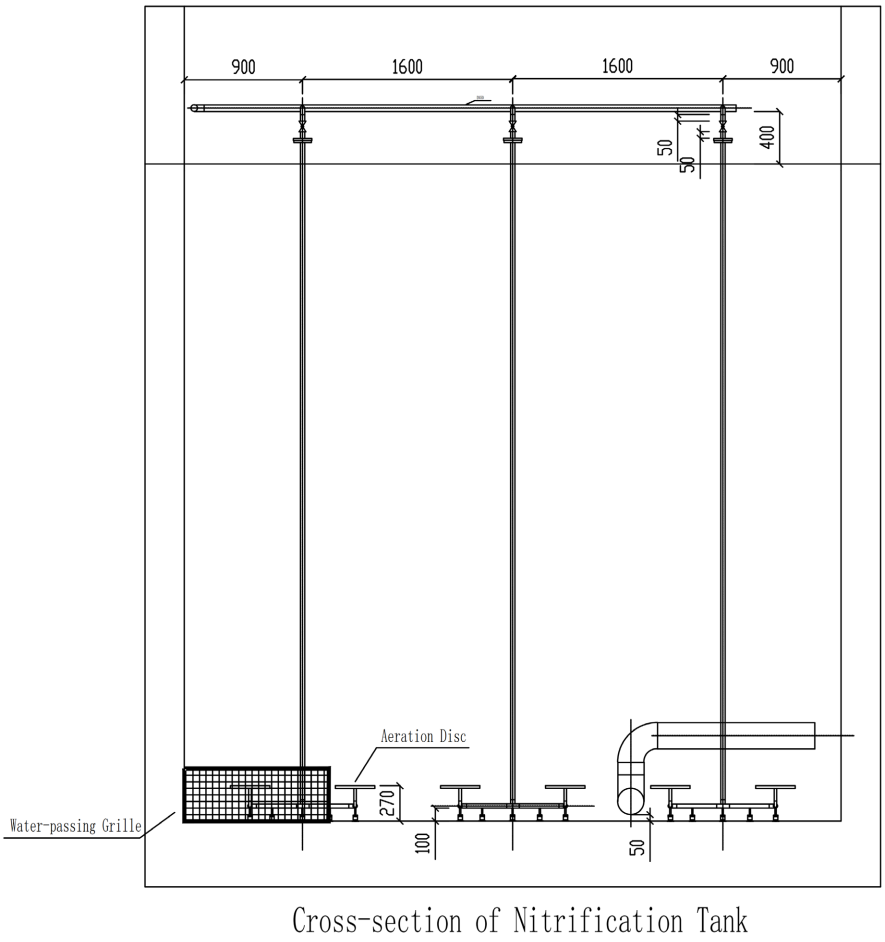

Figure 5. Section diagram of nitrification tank.

Although the system NH_4^+-N removal rate remained relatively stable, the NAR during this period dropped to a minimum of 76.04%. This could be due to temperature inhibiting AOB activity. However, the embedded fillers provided a stable environment for bacterial growth, maintaining biological activity and mitigating the impact of temperature reduction. Moreover, multiple microbial groups worked synergistically, giving the entire system high stability and resistance to temperature shocks. Simulation experiments on the embedded fillers brought back from the site showed they could still maintain a high NAR. During this period, the system experienced sudden flow changes and cooling. However, by day 111, the system effluent NH_4^+-N returned to 0.55 mg/L, indicating normal effluent. Although the water temperature dropped to 8˚C, based on stable effluent quality, the system's treatment capacity was higher compared to the activated sludge process [22]. As shown in **Figure 6**, after the Spring Festival, the influent NH_4^+-N concentration gradually increased, reaching a maximum of 55.43 mg/L. However, despite the continuous rise in influent NH_4^+-N, the NH_4^+-N concentrations in the partial nitrification tank and system effluent remained relatively stable without significant fluctuations.

The overall system's ammonia oxidation rate (AOR) was relatively low, only

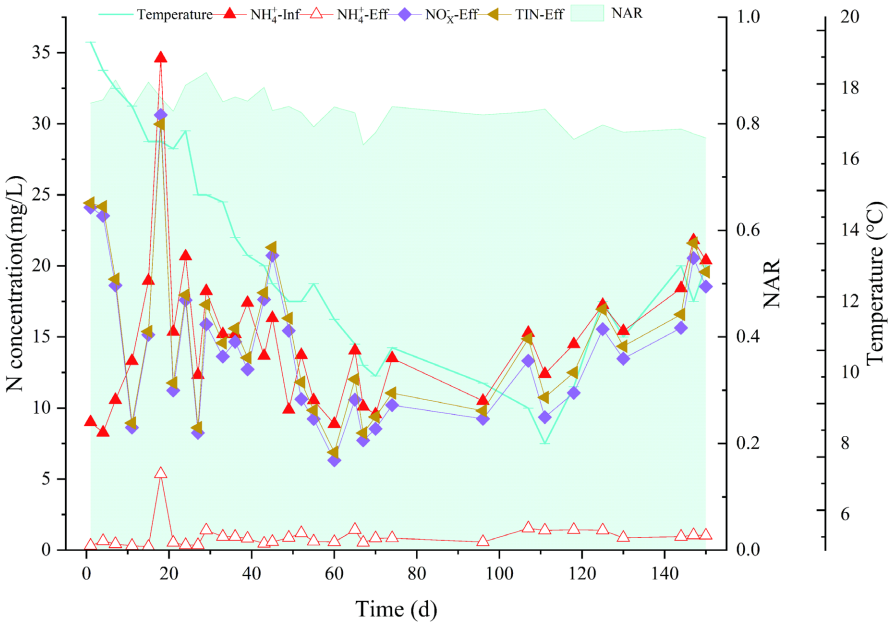

Figure 6. Nitrification tank inlet and outlet water nitrogen concentration changes.

4.915 mg/(L·h), but it achieved a relatively stable partial nitrification process. This might be due to: 1) The embedded immobilized fillers used were partial nitrification fillers enriched with AOB, and MIT significantly reduced biomass loss, maintaining a high AOB abundance, thus enabling partial nitrification; 2) Under low DO conditions, the O_2 mass transfer driving force is smaller. This contradicts the research by Yang Qing *et al.* [23], which suggested high DO could achieve stable partial nitrification, but studies by Blackburne *et al.* and Zhang Gongliang *et al.* [24] [25] achieved high NAR accumulation by controlling low DO. Although both AOB and NOB activity decrease under low DO conditions, AOB has a lower oxygen half-saturation coefficient than NOB [26], giving AOB a competitive advantage over NOB under low DO. According to the microbial community analysis in Section 4, the dominant genus was *Nitrosomonas* (10.82%), a key AOB that maintained high activity even under low-temperature conditions [27]. The intermittent aeration and low DO operation mode employed by the process effectively suppressed nitrite-oxidizing bacteria (NOB), inhibiting their proportion to 1.93%, compensating for the decreased metabolic activity caused by low DO, and enabling a stable partial nitrification phase.

Overall, in the low-temperature environment, this phenomenon was mainly attributed to the high biomass maintained by the immobilization technology and the synergistic promotion of microbial activity by suitable substrate concentration and DO environment. This indicates that the embedded biological fillers possess good resistance to shock loads, effectively buffering influent water quality changes, thereby enhancing the overall operational efficiency and stability of the system.

3.1.2. Denitrification Performance in Winter

On day 1, the NO_x^--N concentration in the primary denitrification tank effluent

was high. At this time, the DO in the nitrification tank was in the range of 3.4 - 4.4 mg/L, and the DO in the recycle flow to the primary denitrification tank was around 2.0 mg/L, which disrupted the anoxic environment for denitrification, leading to poor denitrification performance. The effluent NO_x^--N concentration reached 7.19 mg/L. By day 4, the DO in the denitrification tank was reduced by placing the recycle pump at the bottom end of the nitrification tank (below the aerators). On day 7, the effluent NO_x^--N concentration from the denitrification tank significantly decreased to 3.51 mg/L. On one hand, because the recycle liquid carried less DO, it helped maintain the anoxic environment in the denitrification tank; on the other hand, due to the low C/N ratio of the wastewater, organic matter in the water could not be fully utilized, resulting in residual NO_x^--N in the effluent [28].

Average influent COD = 76.59 mg/L, recycle liquid NO_x^--N = 14.33 mg/L, effluent NO_x^--N = 2.65 mg/L. The theoretical C/N ratio for reducing NO_3^--N is 2.86, and for reducing NO_2^--N it is 1.71 [29]. In this experiment, due to the low NH_4^+-N concentration resulting in fewer electron acceptors provided by the recycle liquid, and the fact that denitrifying bacteria grow thicker biofilms at low temperatures, which might block electron acceptor channels, the effluent NO_x^--N concentration from the primary denitrification tank reached 6.19 mg/L on day 107. This was caused by the accumulation of activated sludge and inadequately intercepted sludge from the influent. After backwashing and sludge removal, the system quickly returned to normal.

To enhance the nitrogen removal capability of the primary denitrification tank, the impact of adjusting the internal recycle ratio on denitrification effectiveness was investigated. Under a 100% internal recycle ratio, the effluent NO_x^--N concentration was 1.61 mg/L, and effluent TIN was 2.06 mg/L. However, residual COD still existed. From day 36, the internal recycle ratio was increased to enhance nitrite/nitrate supply, strengthen mass transfer effects, and stimulate the activity of denitrifying bacteria [30], thereby improving nitrogen removal efficiency and internal carbon source utilization. As shown in **Figure 7**, a significant decrease in effluent NO_x^--N was observed on day 39. To verify whether this result was caused by the recycle ratio adjustment, the internal recycle ratio was restored to 100%. As a result, an increase in effluent NO_x^--N was observed again on day 43. This indicates that under low-temperature conditions, increasing the internal recycle ratio can effectively enhance the system's denitrification capacity.

To further verify the impact of different internal recycle ratios, the internal recycle ratio was increased to 150% starting from day 49. During this phase, the average effluent NO_x^--N concentration from the primary denitrification tank was 2.32 mg/L, slightly lower than the 2.97 mg/L under the 100% recycle ratio condition. However, the average water temperature during the operation period with a 150% recycle ratio was lower, which exerted some inhibitory effect on the metabolic activity of denitrifying bacteria. Nevertheless, because the system employed embedding immobilization technology, which effectively maintained

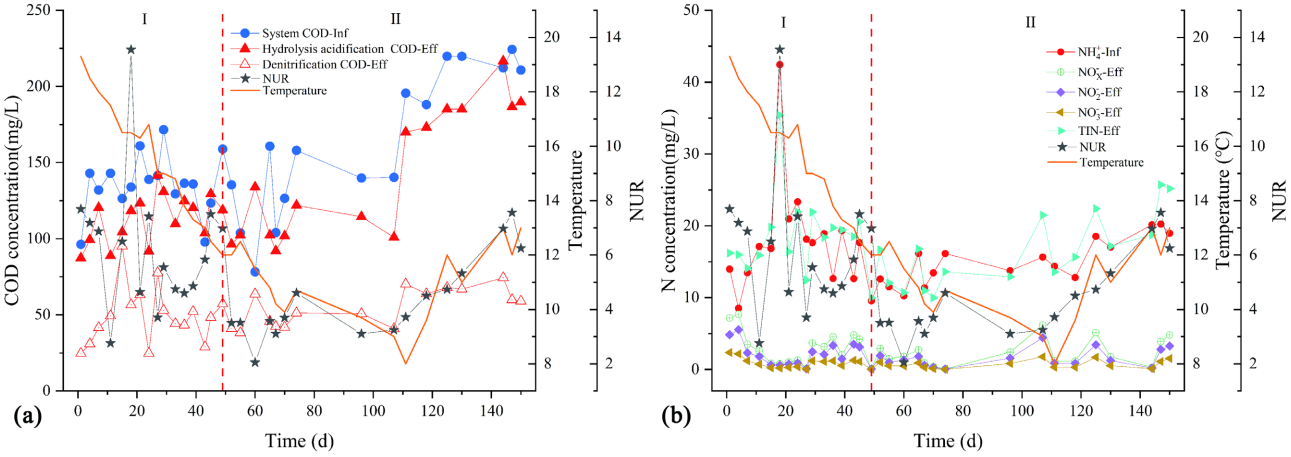

Figure 7. COD and Nitrogen removal effect of the denitrification tank.

microbial performance, the effluent NO_x^--N could still be maintained at a relatively low level.

In summary, under low-temperature operating conditions, the scenario with a 150% internal recycle ratio was superior in terms of nitrogen removal effect compared to maintaining a 100% internal recycle ratio, more effectively enhancing the overall denitrification capacity and carbon source utilization efficiency of the system.

3.2. Changes in Pollutant Concentrations along the Process during Stable System Operation

To observe changes in pollutant concentrations along the process, samples were taken at points along the flow path. The average concentration changes of pollutants over 150 days along the process are shown in **Figure 8**. The transformation processes of pollutants showed similar overall trends in different stages.

After passing through the hydrolysis-acidification tank, the COD concentration decreased significantly, while the NH_4^+-N concentration slightly increased. This phenomenon is highly consistent with the functions of the microorganisms enriched in this functional tank. The dominant phyla in the embedded fillers of this tank were *Bacillota* (19.50%) and *Bacteroidota* (11.29%) (**Figure 9(a)**). These two groups are efficient hydrolysis-acidification bacteria. From the reaction process perspective, complex organic matter in the wastewater first undergoes hydrolysis by extracellular enzymes of hydrolytic bacteria, producing small molecule organic substances that can be utilized by acidogenic bacteria. These substances are further converted into VFAs [31]. This directly led to the decrease in COD and provided carbon sources for subsequent denitrification. Simultaneously, nitrogenous organic matter released ammonia nitrogen during degradation, undergoing ammonification. At the species level, *unclassified_k__norank_d__Bacteria*, *norank_f__Bacteroidetes_vadinHA17*, *Rossellomorea*, and *Trichlorobacter* were the dominant species, accounting for 14.67%, 5.22%, 5.41%, and 4.51% respectively. They play important roles in treating antibiotics, increasing VFAs in the system, enhancing nitrogen and phosphorus removal capacity, removing iron and

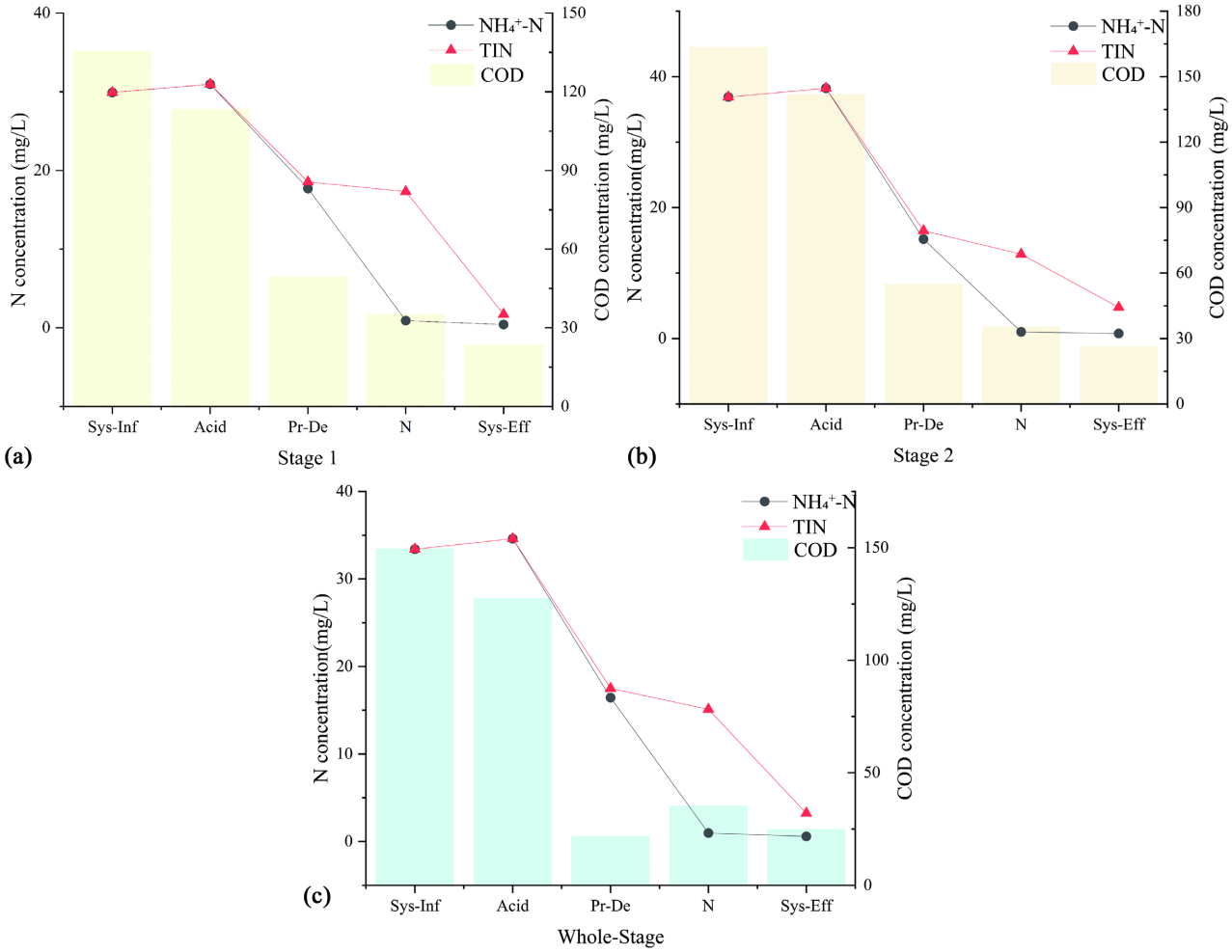

Figure 8. Average concentration variation of pollutants along the process in the system during low-temperature operation period. (a) Variation of pollutant concentrations along the process in Stage I; (b) Variation of pollutant concentrations along the process in Stage II; (c) Variation of pollutant concentrations along the entire process.

manganese from wastewater, degrading cellulose, and improving hydrolysis-acidification efficiency [32]-[35].

The core function of the primary denitrification tank is to use VFAs produced in the hydrolysis-acidification tank as carbon sources to reduce nitrate/nitrite from the recycle flow of the nitrification tank to nitrogen gas. From **Figure 8**, it can be seen that the effluent COD and NO_x^--N concentrations from this unit decreased significantly and simultaneously. In Stage II (R = 150%), this unit's removal effect on NO_x^--N was stronger than in Stage I (R = 100%). Its denitrification performance is inseparable from the special microbial community in this tank. The dominant genus in the embedded fillers of this tank was *Acinetobacter*, accounting for 31.10% (**Figure 9(b)**). *Acinetobacter* is a versatile denitrifying bacterium that can not only use nitrate/nitrite for denitrification but also directly utilize some organic nitrogen sources. This explains why the total nitrogen (TN) loss in this unit is not only from denitrification but may also come from bacterial assimilation.

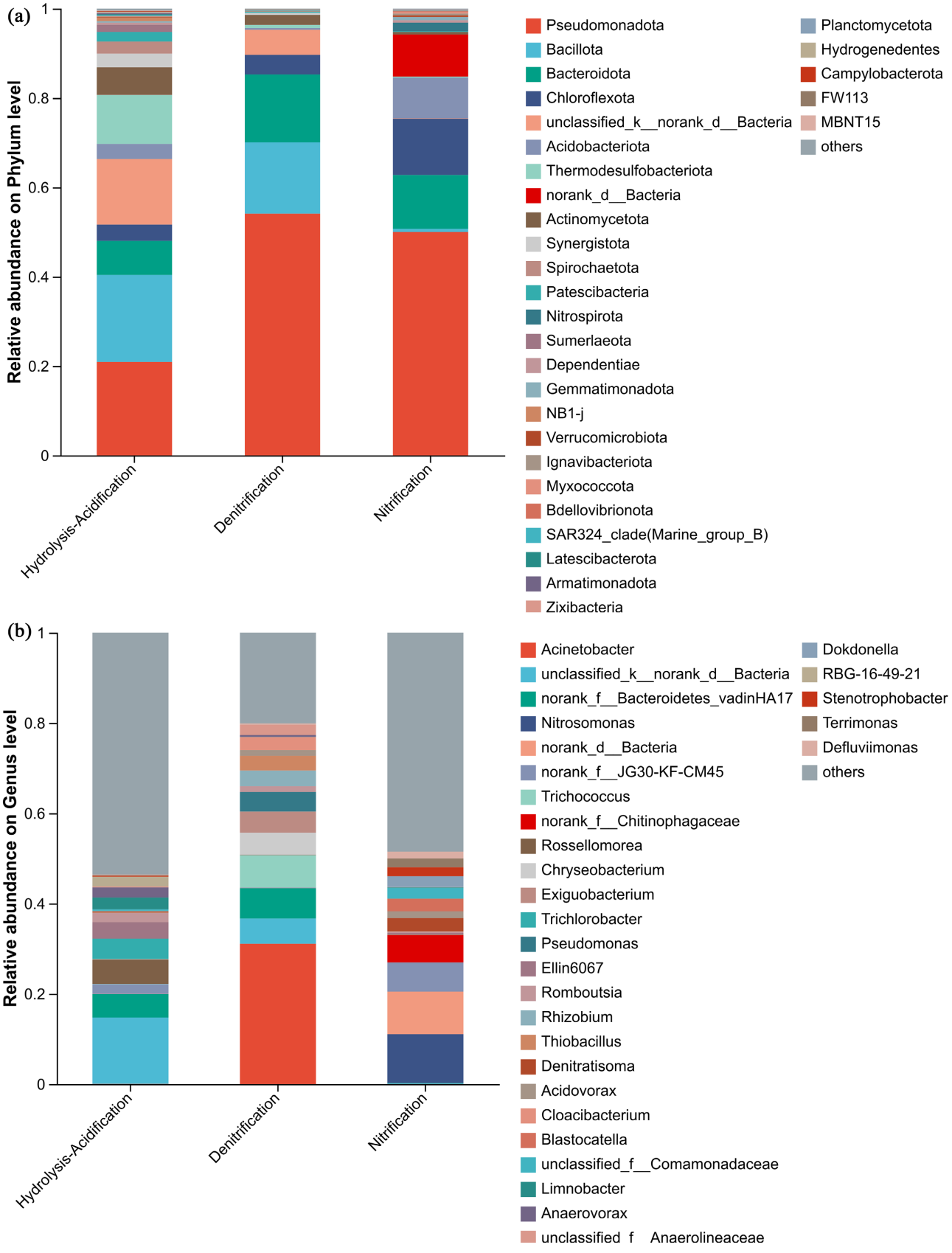

Figure 9. Microbial community and population abundance in functional pool. (a) Phylum level; (b) Genus level.

It can be observed that a decrease in nitrate nitrogen concentration was detected in the nitrification tank. According to 16S rRNA microbial community analysis: besides *Nitrosomonas*, the tank contained relatively high abundances of *norank_f__JG30-KF-CM45* (6.46%), *norank_f__Chitinophagaceae* (6.09%), and *unclassified_k__norank_d__Bacteria* (9.43%), which are non-classical nitrifying bacteria. These bacterial groups can participate in the decomposition of nitrogenous organic matter and possess denitrification capabilities [36]. Therefore, the TIN in the nitrification tank effluent was slightly lower than that of the primary denitrification tank effluent, showing a downward trend in the graph.

When comparing system conditions with recycle ratios of 100% and 150% (**Figure 9(a)**, **Figure 9(b)**), it was found that the TIN was closer to NH_4^+-N at a 100% recycle ratio. This was due to: 1) Prolonged low temperatures between days 50 - 150 led to reduced biological activity. The overall biological activity in Stage II was lower than in Stage I, resulting in incomplete denitrification in the secondary denitrification process; 2) There were certain fluctuations in water quality after the Spring Festival during Stage II. This led to residual NO_x^--N during Stage II, but the effluent TIN still met discharge standards.

For the overall system, under low-temperature conditions, maintaining low DO (3 - 5 mg/L) in the nitrification tank can stabilize AOB growth, and intermittent aeration in a "supply on demand" manner can suppress NOB growth. Simultaneously, increasing the recycle ratio can enhance the denitrification capacity of the primary denitrification tank by providing more substrate. The low DO from the nitrification tank in the recycle liquid to the denitrification tank also helps maintain low DO, preserving the anoxic state in the denitrification tank, creating conditions for denitrifying bacteria growth, and enhancing the overall system's nitrogen removal performance.

4. Microbial Analysis

High-throughput sequencing technology was used to perform 16S rRNA sequencing on ammonia-oxidizing sludge before and after acclimation and enrichment to explore changes in microbial diversity. Test samples were stored in a low-temperature refrigerator before being sent for testing. The microbial diversity sequencing results are shown in **Table 3**.

Table 3. Diversity index sequencing results.

Sample	Coverage	ACE	Simpson
Hydrolysis-Acidification	0.99644	1137.49598	0.01579
Denitrification	0.99678	716.8188	0.04499
Nitrification	0.99718	774.59314	0.02311

The Simpson index reflects the microbial population diversity in the tested samples; a higher value indicates lower microbial diversity and stronger concentration. Higher microbial abundance in the system enhances resistance to drastic

environmental changes. The data in the table precisely indicate that embedding immobilization technology can ensure the population stability of dominant species, making their leading role evident.

At the phylum classification level (**Figure 9(b)**), the microbial community structures of the three functional tanks differed significantly and were closely associated with their respective process functions. *Pseudomonadota* played an important role in all three tanks, especially becoming the dominant phylum in the denitrification tank (54.11%) and partial nitrification tank (50.00%). This phylum contains many key bacterial species with nitrogen metabolism functions. *Bacillota* reached an abundance of 19.50% in the hydrolysis-acidification tank; this group is a core phylum for hydrolysis and fermentation producing VFAs [37]. *Bacteroidota* also had relatively high abundances in the denitrification tank (15.20%) and hydrolysis-acidification tank (11.29%), participating in organic matter degradation and improving carbon source utilization efficiency [38]. The relatively high proportions of *Planctomycetota* (8.43%) and *Chloroflexi* (7.08%) in the partial nitrification tank indicate complex microbial synergistic relationships.

The synergy of multiple microbial groups reflects the complexity of rural wastewater and highlights the importance of the hydrolysis-acidification tank. It not only hydrolyzes complex organic matter into simpler organic matter but also contributes to energy saving, sludge reduction, and shock resistance, reducing the operating costs and maintenance difficulty of wastewater tanks, making it highly suitable for rural wastewater treatment. Furthermore, even as water temperature decreased, microorganisms could maintain activity and COD degradation efficiency within the stable microenvironment constructed by embedding immobilization technology, demonstrating good operational stability of the system.

5. Conclusions

1) Under low-temperature conditions, the synergistic effect of each functional unit in the system resulted in excellent treatment efficiency and strong stability. During the low-temperature period of 8˚C - 19.3˚C, MIT technology showed significant treatment effects for low C/N rural wastewater: NH_4^+-N and COD removal rates reached 93.43% and 82.25%, respectively; NAR remained around 82.8%; average effluent NH_4^+-N and COD were 0.65 mg/L and 24.97 mg/L, respectively, meeting and exceeding relevant discharge standards. The hydrolysis-acidification tank efficiently provided VFAs as effective carbon sources for subsequent denitrification without requiring sludge recycle. The partial nitrification tank effectively suppressed nitrite-oxidizing bacteria (NOB, accounting for only 1.93%) by controlling DO. The core AOB (*Nitrosomonas*, accounting for 10.82%) maintained activity even at 8˚C, resulting in excellent partial nitrification stability. After increasing the internal recycle ratio to 150% in the primary denitrification tank, the average effluent NO_x^--N decreased to 2.32 mg/L, contributing 65% to total nitrogen removal.

2) The microbial diversity and community structure in each functional unit

showed distinct advantages: The hydrolysis-acidification tank had the highest ACE index (1137.496), conducive to maintaining microbial diversity. The dominant phylum *Bacillota* (19.50%) could efficiently degrade macromolecular organic matter to produce VFAs. The denitrification tank had the highest Simpson index (0.045), indicating concentrated dominant microbial groups. The core genus *Acinetobacter* (31.10%) could utilize various nitrogen sources for efficient denitrification. The dominant phylum in the partial nitrification tank, *Pseudomonadota* (50.00%), contained core AOB, ensuring low-temperature ammonia oxidation efficiency.

3) Compared to traditional wastewater treatment processes, MIT technology has advantages such as high biomass, resistance to microbial washout, and tolerance to environmental fluctuations. It better meets the low-cost and easy operation and maintenance requirements for decentralized rural wastewater treatment, showing broad application prospects.

Conflicts of Interest

The authors declare no conflicts of interest.

References

[1] Ministry of Ecology and Environment of the People's Republic of China (2025) 2024 China Ecological and Environmental Status Bulletin. https://www.mee.gov.cn/ywgz/sthjjcgl/hjzljcypj/202506/t20250605_1120773.shtml

[2] Xie, L.H., Wu, D.L. and Zhang, Y.L. (2018) Analysis and Evaluation of the Current Situation of Rural Domestic Sewage Treatment Technology in China. *Journal of Ecology and Rural Environment*, **34**, 865-870.

[3] Jiang, H.J. and Xu, C.X. (2025) Analysis on the Current Situation and Countermeasures of Rural Domestic Sewage Treatment. *Rural Practical Technology*, No. 6, 113-114.

[4] Xing, P., Wang, Z.X., Xian, Y., Duan, H.B., Zhao, H.L. and Qin, X.Z. (2025) Research Status and Trend of Rural Domestic Sewage Treatment in China. *Environmental Ecology*, **7**, 74-82.

[5] Guo, F., Chen, Y., Wang, G.T., *et al.* (2022) Current Situation, Problems and Development Suggestions of Rural Domestic Sewage Treatment in China. *Water Supply and Drainage*, No. S1, 68-72.

[6] The State Council of the People's Republic of China (2021) Outline of the 14th Five-Year Plan for National Economic and Social Development of the People's Republic of China and Vision 2035. http://www.gov.cn/xinwen/2021-03/13/content_5592681.htm

[7] Bai, Y.M. and Li, H.Y. (2024) Research Progress of Decentralized Rural Sewage Treatment Technology. *Cleaning World*, **40**, 89-91.

[8] Kuang, W., Wang, X.Y., Zhou, Q.Y., *et al.* (2015) Improve the Removal Efficiency of TN in Rural Domestic Sewage with low C/N Value. *Environmental Engineering*, **9**, 4252-4258.

[9] Hao, R.J., Zheng, J.Y., Han, S.W., *et al.* (2023) Experimental Study on Low C/N Rural Domestic Sewage Treatment. *Environmental Science*, **42**, 50-54.

[10] Kaiser, A.S., Fernández, V., Claria, I., *et al.* (2016) Hydraulic Characterization of an

Activated Sludge Reactor with Recycling System by Tracer Experiment and Analytical Models. *Water Research*, **95**, 195-204.

[11] Jia, Y., Zhou, M., Chen, Y., Hu, Y. and Luo, J. (2020) Insight into Short-Cut of Simultaneous Nitrification and Denitrification Process in Moving Bed Biofilm Reactor: Effects of Carbon to Nitrogen Ratio. *Chemical Engineering Journal*, **400**, Article ID: 125905. https://doi.org/10.1016/j.cej.2020.125905

[12] Hu, J., Wang, J., Li, X., Zhao, J., Liu, W. and Zhu, C. (2024) Efficient Nitrogen Removal and Substrate Usage in Integrated Fixed-Film Activated Sludge-Anammox System under Seasonal Temperature Variation. *Bioresource Technology*, **391**, Article ID: 129946. https://doi.org/10.1016/j.biortech.2023.129946

[13] Liu, W., Chu, Y., Tan, Q., Chen, J., Yang, L., Ma, L., *et al.* (2022) Cold Temperature Mediated Nitrate Removal Pathways in Electrolysis-Assisted Constructed Wetland Systems under Different Influent C/N Ratios and Anode Materials. *Chemosphere*, **295**, Article ID: 133867. https://doi.org/10.1016/j.chemosphere.2022.133867

[14] Zhou, X., Wang, X., Zhang, H. and Wu, H. (2017) Enhanced Nitrogen Removal of Low C/N Domestic Wastewater Using a Biochar-Amended Aerated Vertical Flow Constructed Wetland. *Bioresource Technology*, **241**, 269-275. https://doi.org/10.1016/j.biortech.2017.05.072

[15] Wang, Y., Zhang, B., Tang, C., *et al.* (2016) Multistage Vertical-Flow Constructed Wetlands and Removal Efficiency of Nitrogen and Phosphorus in Cold Area. *Transactions of the Chinese Society of Agricultural Engineering*, **32**, 200-205.

[16] Chen, M.F., Peng, Z.Y., Jiang, Q.M., *et al.* (2020) Preparation of Embedded Granules of Activated Sludge and Its Ammonia Nitrogen Treatment Performance. *Journal of Environmental Engineering Technology*, **14**, 2926-2933.

[17] Yang, H., Xu, F., Meng, C., *et al.* (2018) Rapid Improvement of Denitrification Performance and Community Analysis of Embedded Activated Sludge. *Environmental Science*, **39**, 4651-4659.

[18] Kong, H.X. (2025) Sodium Alginate-Zeolite Embedded AnAOB Enhanced PD-Anammox Denitrification Efficiency and Influencing Factors. *Water Purification Technology*, **44**, 85-92, 128.

[19] State Environmental Protection Administration of China (2002) Methods for Monitoring and Analysis of Water and Wastewater. 4th Edition, China Environmental Science Press, 323-334.

[20] Li, H.P., Pang, W.H., Xie, L., *et al.* (2022) Characteristics and Transformation Analysis of Organic Carbon Sources in Low C/N Wastewater Treatment Process. *China Water & Wastewater*, **38**, 69-74.

[21] Ai, W., Shang, J., Wang, Y., *et al.* (2025) Constructing a Robust Mainstream Anammox Process via Cold Shock Adaptation: Nitrogen Removal Performance and Microbial Community. *Journal of Environmental Chemical Engineering*, **13**, Article ID: 119443. https://doi.org/10.1016/j.jece.2025.119443

[22] Liu, X., Zeng, A., Wang, Y., Liu, P., Chen, Y. and Jiang, Y. (2018) Comparison and Strategy of Nitrogen Removal at Different Low Temperatures in a Pilot-Scale A^2/O System. *Environmental Technology*, **40**, 2473-2481. https://doi.org/10.1080/09593330.2018.1444099

[23] Yang, Q., Yang, Y.B., Yang, Z.Q., *et al.* (2018) Effect of Dissolved Oxygen on Short-Cut Nitrification Stability and Functional Bacteria. *China Environmental Science*, **38**, 3328-3334.

[24] Blackburne, R., Yuan, Z. and Keller, J. (2007) Partial Nitrification to Nitrite Using Low Dissolved Oxygen Concentration as the Main Selection Factor. *Biodegradation*,

19, 303-312. https://doi.org/10.1007/s10532-007-9136-4

[25] Zhang, G.L., Li, D., Zhang, X.J., *et al.* (2014) Experimental Study on the Stability of Shortcut Nitrification in SBR with Low Temperature and Low Ammonia Nitrogen. *China Environmental Science*, **34**, 610-616.

[26] Picioreanu, C., Perez, J. and van Loosdrecht, M.C.M. (2016) Impact of Cell Cluster Size on Apparent Half-Saturation Coefficients for Oxygen in Nitrifying Sludge and Biofilms. *Water Research*, **106**, 371-382. https://doi.org/10.1016/j.watres.2016.10.017

[27] Urakawa, H., Tajima, Y., Numata, Y. and Tsuneda, S. (2008) Low Temperature Decreases the Phylogenetic Diversity of Ammonia-Oxidizing Archaea and Bacteria in Aquarium Biofiltration Systems. *Applied and Environmental Microbiology*, **74**, 894-900. https://doi.org/10.1128/aem.01529-07

[28] Hou, H.J., Wang, H.Y. and Zhou, Q. (2005) Effects of Influent COD Concentration and C/N Ratio on Nitrogen Removal. *China Water & Wastewater*, **21**, 30-34.

[29] Li, Y. (2017) Water Supply and Drainage Design Manual: Volume 5 Urban Drainage. 3rd Edition, China Architecture & Building Press.

[30] Zhang, L.C., Peng, Y.Z., Wang, J.H., *et al.* (2011) Effect of Internal Circulation on Nitrogen and Phosphorus Removal Characteristics of A^2/O-Biological Aerated Filter Process. *Environmental Science*, **32**, 159-165.

[31] Li, S., Yang, H. and Chen, Y. (2024) Use of Embedding Immobilized Biofillers to Improve Hydrolysis Acidification Efficiency in Domestic Wastewater Treatment. *Bioresource Technology*, **414**, Article ID: 131631. https://doi.org/10.1016/j.biortech.2024.131631

[32] Tian, J., Chen, C., Lartey-Young, G. and Ma, L. (2023) Biodegradation of Cefalexin by Two Bacteria Strains from Sewage Sludge. *Royal Society Open Science*, **10**, Article ID: 220442. https://doi.org/10.1098/rsos.220442

[33] Wang, R., Li, C., Lv, N., Pan, X., Cai, G., Ning, J., *et al.* (2021) Deeper Insights into Effect of Activated Carbon and Nano-Zero-Valent Iron Addition on Acidogenesis and Whole Anaerobic Digestion. *Bioresource Technology*, **324**, Article ID: 124671. https://doi.org/10.1016/j.biortech.2021.124671

[34] Lee, W.S., Aziz, H.A. and Tajarudin, H.A. (2023) Removal of Fe and Mn from the Groundwater by Using Zeolite with *Rossellomorea* Sp. *Water Environment Research*, **95**, e1330. https://doi.org/10.1002/wer.10913

[35] Yousef, N.M.H., Danial, A.W. and Mawad, A.M.M. (2024) Fermentative Bioconversion of Non-Pretreated Wheat Bran to Hydrogen via Cellulolytic *Rossellomorea marisflavi* and Role of Calcium Oxide Nanoparticles for Enhancement Gas Productivity. *Waste and Biomass Valorization*, **15**, 3255-3268. https://doi.org/10.1007/s12649-023-02373-4

[36] Jiang, Y.B., Ling, W., Wei, C.Z., *et al.* (2022) Study on Nitrogen Removal Performance and Functional Bacteria of Rural Domestic Sewage Treatment Process Enhanced by Composite Solid Carbon Source. *Environmental Engineering*, **40**, 62-70.

[37] Grana, M., Catenacci, A. and Ficara, E. (2023) Denitrification Capacity of Volatile Fatty Acids from Sludge Fermentation: Lab-Scale Testing and Full-Scale Assessment. *Fermentation*, **10**, Article 25. https://doi.org/10.3390/fermentation10010025

[38] Long, Y., Ma, Y., Wan, J., Wang, Y., Tang, M., Fu, H., *et al.* (2023) Denitrification Efficiency, Microbial Communities and Metabolic Mechanisms of Corn Cob Hydrolysate as Denitrifying Carbon Source. *Environmental Research*, **221**, Article ID: 115315. https://doi.org/10.1016/j.envres.2023.115315